Biology of Reproduction, 2018, 99(3), 578–589
doi:10.1093/biolre/ioy079
Research Article
Advance Access Publication Date: 4 April 2018

Research Article

Sox17 is essential for proper formation of the marginal zone of extraembryonic endoderm adjacent to a developing mouse placental disk†

Hitomi Igarashi[1], Mami Uemura[1,2], Ryuji Hiramatsu[1], Ryuto Hiramatsu[1], Saki Segami[1], Montri Pattarapanawan[1], Yoshikazu Hirate[2], Yuki Yoshimura[3], Haruo Hashimoto[3], Hiroki Higashiyama[1], Hiroyuki Sumitomo[1], Masamichi Kurohmaru[1], Yukio Saijoh[4], Hiroshi Suemizu[3], Masami Kanai-Azuma[2] and Yoshiakira Kanai[1,*]

[1]Department of Veterinary Anatomy, The University of Tokyo, Bunkyo-ku, Tokyo, Japan; [2]Department of Experimental Animal Model for Human Disease, Center for Experimental Animals, Tokyo Medical and Dental University, Bunkyo-ku, Tokyo, Japan; [3]Central Institute for Experimental Animals, Kawasaki-ku, Kawasaki, Kanagawa, Japan and [4]Department of Neurobiology and Anatomy, The University of Utah, Salt Lake City, Utah, USA

*__Correspondence:__ Department of Veterinary Anatomy, The University of Tokyo, Yayoi 1-1-1, Bunkyo-ku, Tokyo 113-8657, Japan. Tel: 81-3-5841-5384; Fax: 81-3-5841-8181; E-mail: aykanai@mail.ecc.u-tokyo.ac.jp:

†__Grant Support:__ This work was supported by financial grants from the Ministry of Education, Science, Sports and Culture of Japan to Y. Kanai (S-24228005) and M. Kanai-Azuma (B-15H04282), and from the National Institute of Health to Y Saijoh (HL107152).
Edited by Dr. Myriam Hemberger, PhD, Babraham Institute

Received 24 January 2018; Revised 15 March 2018; Accepted 3 April 2018

Abstract

In mouse conceptus, two yolk-sac membranes, the parietal endoderm (PE) and visceral endoderm (VE), are involved in protecting and nourishing early-somite-stage embryos prior to the establishment of placental circulation. Both PE and VE membranes are tightly anchored to the marginal edge of the developing placental disk, in which the extraembryonic endoderm (marginal zone endoderm: ME) shows the typical flat epithelial morphology intermediate between those of PE and VE in vivo. However, the molecular characteristics and functions of the ME in mouse placentation remain unclear. Here, we show that SOX17, not SOX7, is continuously expressed in the ME cells, whereas both SOX17 and SOX7 are coexpressed in PE cells, by at least 10.5 days postconception. The *Sox17*-null conceptus, but not the *Sox7*-null one, showed the ectopic appearance of squamous VE-like epithelial cells in the presumptive ME region, together with reduced cell density and aberrant morphology of PE cells. Such aberrant ME formation in the *Sox17*-null extraembryonic endoderm was not rescued by the chimeric embryo replaced with the wild-type gut endoderm by the injection of wild-type ES cells into the *Sox17*-null blastocyst, suggesting the cell autonomous defects in the extraembryonic endoderm of *Sox17*-null concepti. These findings provide direct evidence of the crucial roles of SOX17 in proper formation and maintenance of the ME region, highlighting a novel entry point to understand the in vivo VE-to-PE transition in the marginal edge of developing placenta.

Summary Sentence

The marginal extraembryonic endoderm adjacent to a developing placental disk continuously expresses SOX17 during mouse placentation; its aberrant formation was observed in *Sox17*-null but not *Sox7*-null concepti in the pregnant uterus.

Key words: SOX17, conceptus, placentation, transcriptional regulation, rodents.

Introduction

After implantation, each embryo in the rodent gastrula is surrounded by two extraembryonic endoderm layers, the visceral endoderm (VE) and the parietal endoderm (PE), inside the mother's uterus. VE cells cover the proximal parts of the extraembryonic region and provide a continuous link to the embryonic gut endoderm at the distal region of the embryonic side. In contrast, the outer PE cells are underlain by a single thick layer of basal lamina, Reichert membrane [1–4]. These two endoderm layers are involved in protecting and nourishing the embryo at the maternal–fetal interface, especially before the establishment of placental circulation (approximately 10.5 days postconception [dpc] in mice). During gastrulation and organogenesis stages prior to placental establishment, two PE and VE layers are anatomically anchored and linked via the marginal zone endoderm (ME) lining along the marginal edge of the ectoplacental cone/chorionic plate of the developing placental disk [5]. The ME displays a morphology intermediate (i.e. a gradient hybrid character) between those of PE and VE cells at the junction between them. It was previously speculated that, near the ME region, VE cells may relocate to transdifferentiate into PE cells [6, 7]. However, the molecular characteristics and functions of the ME at early stages of organogenesis remain unclear [8].

Sox17 and *Sox7*, two members of the *Sry*-related High mobility group (HMG) box gene F (SoxF) subgroup, together with *Sox18*, were previously shown to be activated and involved in the primitive endoderm (PrE) and its derivatives at the blastocyst stage and subsequent implantation stages [9–12]. In vitro functional analyses of the role of *Sox17* in the differentiation of PrE from ES cells and PrE-derived stem (XEN) cells indicated that SOX17 acts in an autoregulatory and feedforward network of the extraembryonic endoderm lineage in mice [12–16]. SOX17 alone is also involved in the maintenance of PrE epithelial integrity in vivo, whereas its absence leads to premature delamination and migration of PE [11]. The recovery of redundant SOX7 activity leads to the proper development of PrE, which subsequently results in proper formation of the extraembryonic endoderm layer (i.e. VE and PE) in mouse *Sox17*-null concepti. However, at later stages, despite *Sox17* and *Sox7* expression in some of the proximal extraembryonic endoderm [9], their in vivo function during placentation remains unclear.

In this study, we examined *Sox17* and *Sox7* expression profiles in the proximal extraembryonic endoderm around a developmental placental disk during 7.5–10.5 dpc. Moreover, we examined and compared the phenotypes of *Sox17*-null and *Sox7*-null concepti, as well as those of *Sox17*-null concepti rescued by the injection of wild-type ES cells into the blastocyst in vivo. The present study provides the first in vivo evidence of the crucial roles of SOX17 in the proper formation and maintenance of the ME region adjacent to the developing placental disk.

Materials and methods

Animals and chimeric embryos

Concepti with placental disks at 7.5–10.5 dpc were obtained from pregnant *Sox17* or *Sox7* heterozygous female mice mated with each heterozygous male ($Sox17^{+/-}$ line [9]; $Sox17^{+/-(Gfp)}$ line [17] [ICR/C57BL6 (B6)-mixed background]; three $Sox7^{+/-}$ lines [B6 background] established by CRISPR/Cas9 in this study [see Supplemental Figure S1]). In some pregnant mothers, EdU (0.2 mg/g body weight) was intraperitoneally injected just 2 h prior to the uterine sampling. A wild-type conceptus with a placental disk was also used in this study for whole-mount in situ hybridization and immunohistochemical analyses of in vivo SOX17 and SOX7 expression profiles. Chimeric *Sox17*-null concepti with wild-type ES cells at 9.5 dpc were also generated by the injection of $Sox17^{+/+}$; *Gfp* + ES cells [18] into $Sox17^{-/-}$ blastocysts [9]. All animal experiments were performed in strict accordance with the Guidelines for Animal Use and Experimentation as established by the University of Tokyo (approval ID: P13-763, P14-877), the Tokyo Medical and Dental University (approval ID: 0160024C2), the Central Institute for Experimental Animals (approval ID: 14050A), and the University of Utah (approval ID: 14-01003).

Loss-of-function *Sox7* mutant lines established by the CRISPR/Cas9 system

A pair of oligos targeting *Sox7* were annealed and inserted into the BsaI site of the pDR274 vector (Addgene), as described by Hashimoto and Takemoto [19]. *Cas9* mRNA and short guide RNAs targeting *Sox7* were introduced into fertilized eggs collected from C57BL/6 females. Three *Sox17*-null lines with frame-shift mutations (4-, 28-, or 31-bp deletion just upstream of the first alpha helices of the HMG box domain, resulting in a complete lack of its HMG box domain) were established by backcrossing C57BL/6 wild-type mice (Supplemental Figure S1A). In this study, we mainly used the 28-bp deletion line for *Sox7*-mutant analyses. In all these three lines, embryonic lethality was revealed in *Sox7*-null embryos at around 10.5 dpc, showing a typical phenotype with a lack of blood vessels in the yolk sac (Supplemental Figure S1B and C; [20–22]). Similar to such lethal phenotypes of *Sox7*-null embryos, the *Sox17*-null embryos also showed embryonic lethality at around 10.5 dpc due to cardiovascular defects with no axis rotation (i.e. no embryonic turning; [9, 23, 24]).

Whole-pregnant-uterus analysis and conceptus genotyping

The whole uterus, including the conceptus, placental disk, endometrium, myometrium, and perimetrium, was dissected into each two-conceptus part of the whole uterine tube, followed by direct fixing with Bouin solution or 4% paraformaldehyde-phosphate

buffered saline (PFA-PBS) for routine preparation of serial paraffin sections (Supplemental Figure S2A and B). Each genotype of the conceptus within the uterus was evaluated by anti-SOX17 or SOX7 immunostaining. In brief, the presence (wild type or +/−) or absence (−/−) of each positive signal was monitored in the PE cells of each conceptus (Supplemental Figure S2C and D), in addition to the reference staining of anti-GFP signals for the null allele in the whole-uterus sections of the *Sox17*$^{+/-(Gfp)}$ line. In all the whole-pregnant-uterus samples, either the heterozygote/wild-type or the null genotype was also reconfirmed by the appearance or presence of the typical phenotypes of the *Sox17*-null embryos (no axis rotation with defective hindgut formation; see also Supplemental Figure S2B) or *Sox7*-null embryos (vascular defects in the yolk sac; see also Supplemental Figure S1B).

As for the isolated concepti including extraembryonic endoderm, the genotype of the *Sox17* or *Sox7* allele was analyzed by polymerase chain reaction using embryonic tissues (*Sox17* as described by Kanai-Azuma [9]; Kim [17]; *Sox7* using the following primers: forward: 5′-TGG CCC GAA GCT GAT AAA TAA GGG-3′; reverse: 5′-TAG AAT TCT TTC CGA ACA GCG TTG TCA C-3′).

Whole-mount in situ hybridization

Whole-mount in situ hybridization of the whole concepti with placental disk was performed as described previously [9, 23]. RNA probes for *Sox17* [9], *Sox7*, and *Sox18* [25] were used in this study. Some whole-mount stained samples were refixed in 4% PFA-PBS and then serially cryosectioned (7–8 μm in thickness).

Histology and immunohistochemistry

For paraffin sections, a whole pregnant uterus or isolated conceptus with placental disk was fixed in 4% PFA-PBS or Bouin solution for 12 h at 4°C, dehydrated, embedded in paraffin, and then serially sectioned (4 μm in thickness). The sections were incubated with anti-cadherin1 (CDH1; previously known as E-cadherin) (1:400 dilution; Cell Signaling Technology), anti-GATA binding protein 6 (GATA6; 1:100 dilution; R&D Systems), anti-GFP (1:200 dilution; MBL), anti-hepatic nuclear factor 4, alpha (HNF4a; 1:400 dilution; Santa Cruz Biotechnology), anti-SOX17 (1:200 dilution; R&D Systems), anti-SOX7 (1:200 dilution; R&D Systems), or anti-phosphorylated-ezrin/radixin/moesin (p-ERM) antibody (1/100 dilution; Cell Signaling Technology; Supplementary Table1). Finally, the immunoreaction was visualized using biotin-conjugated secondary antibody in combination with an ABC Kit (Vector Laboratories; brown staining) or using secondary antibodies conjugated with Alexa-488/594 (green/red fluorescence).

For plastic semithin sections, placental tissues with PE and VE layers were fixed in 2.5% glutaraldehyde/0.1 M phosphate buffer (PB) for 4 h at 4°C. After washing with phosphate-buffered saline (PBS), they were postfixed in 1% OsO_4 in 0.1 M PB for 2 h at 4°C. Then, they were dehydrated and embedded in EPON812, and semi-thin sections (1 μm in thickness) were stained with toluidine blue.

Morphometric and cell proliferation assays

In the stained sections including the maximum placental area of whole-uterus samples (9.5 dpc; more than three sections including maximum placental area per conceptus), the numbers of epithelial endoderm cells just beneath the placental disk (except for the PE cells) were separately calculated in the *Sox17*/*Sox7*-null conceptus and its wild-type/heterozygote (normal) littermates within the uterus. Moreover, random images of the PE region were obtained in the HE-stained sections of whole-uterus samples, and then both the number of PE cells and the length of Reichert membrane were calculated using ImageJ 1.48V software (National Institutes of Health, Bethesda, MD) to determine the density of PE cells (cell number per mm length) in each genotype. To analyze the proliferative activity, the EdU-positive indices of VE and PE cells were also estimated in *Sox17*-null and wild-type/heterozygote (normal) concepti.

Statistical analysis

Quantitative data (i.e. cell numbers, EdU-positive indices, and cell process numbers) are presented as the mean ± SEM (standard error of the mean). Statistical significance was calculated using Student *t*-test, and a *p*-value of 0.05 or less was used to define statistical significance for each analysis.

Results

Sox17 expression is continuously maintained in the ME anchoring to the developing placental disk

The PE and VE are continuously connected via the ME at the proximal site underneath the marginal edge of the trophectoderm-derived placental primordium of the ectoplacental cone/chorionic plate [5]. To define the region of *Sox17* expression in the extraembryonic endoderm, we first examined the spatiotemporal pattern of *Sox17* expression in wild-type concepti by whole-mount in situ hybridization during 7.5–9.5 dpc (Figure 1). Strong *Sox17*-positive signals were detectable in the PE and proximal VE regions directly facing the ectoplacental region (bar in Figure 1A), as well as in the anterior definitive endoderm (red star in Figure 1A and B). In early-to-late somite stages, such *Sox17* signals in the proximal VE region were restricted to ME at the junction between the VE and PE facing the chorionic plate (Figure 1C and D). High *Sox17* signals were maintained in the ME and PE regions at and after 9.5 dpc (Figure 1E and F, and figure not shown). In contrast, in the VE region, *Sox17*-positive signals were clearly reduced to an undetectable level in a distal-to-proximal manner in the VE region during 7.5–9.5 dpc (lower left insets in Figure 1D and F). These findings suggest that *Sox17* expression is continuously maintained in the ME and PE by the late organogenic stages. On the other hand, *Sox7*-positive signals were detected in the ME and PE regions but not in the distal VE region (Figure 1G and H), showing similarity to the *Sox17* expression profile (Figure 1C and D). No *Sox18*-positive signals were detectable in the extraembryonic endoderm, VE, ME, or PE (Figure 1I and J), although its positive signals, as well as those of *Sox17* and *Sox7*, were found in the developing vasculature of the allantois ("AL" in Figure 1C, D, and G–J). Such coexpression profiles of *Sox17* and *Sox7* in the extraembryonic endoderm are consistent with previous data obtained at the early stages of gastrulation [9, 11].

Comparative immunohistochemistry using anti-SOX17 and anti-SOX7 antibodies confirmed the coexpression of SOX17 and SOX7 in the PE at 7.5–10.5 dpc (Figures 2A–D). Neither SOX17- nor SOX7-positive signals were detectable in the distal VE region, which is consistent with the present in situ hybridization data (Figure. 1). Interestingly, the intensity of the SOX17-positive signals in the proximal VE region including the ME was similar to that in the PE within the same conceptus (broken lines in upper plates in Figure 2A–D). In contrast, the intensities of the SOX7 signals appeared lower in the proximal VE and ME regions than in the PE region at 7.5 dpc, and these signals were then clearly reduced in intensity in the ME region

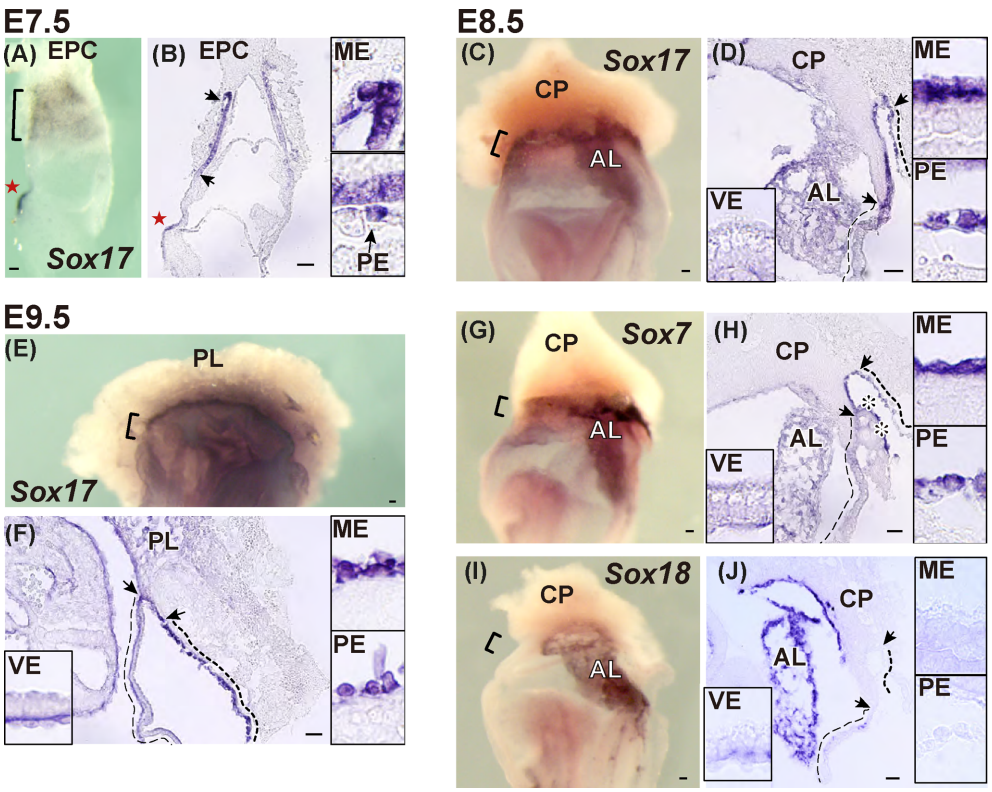

Figure 1. Whole-mount in situ hybridization analyses for high-level *Sox17* expression in the marginal zone endoderm (ME) anchored to the developing placenta. (A–J) *Sox17* expression profiles in the proximal extraembryonic endoderm region near the marginal edge of the developing placental disk at 7.5 (A, B), 8.5 (C, D), and 9.5 dpc (E, F). The expression patterns of *Sox7* and *Sox18* at 8.5 dpc are also shown in G–J. Plates A, C, E, G, and I show whole-mount views of the conceptus with the developing placental disk. Plates B, D, F, H, and J display sagittal sectioning views of whole-mount stained concepti (insets, higher magnification images of PE, VE, and ME). Arrows mark both ends of the *Sox17*-positive ME region. Faint and bold broken lines indicate the VE and PE regions, respectively. Asterisks, nonspecific staining; AL, allantois; CP, chorionic plate; EPC, ectoplacental cone; ME, marginal zone endoderm; PE, parietal endoderm; PL, placental disk; VE, visceral endoderm. Bar, 50 μm.

at and after 8.5 dpc (lower plates in Figure 2A–D). These findings indicate that there is predominant SOX17 expression in the ME region at and after 8.5 dpc in addition to coexpression of SOX17 and SOX7 in PE cells at least by placental establishment (Figure 2E).

Aberrant morphology of the extraembryonic endoderm of the presumptive ME region in *Sox17*-null conceptus

First, we examined the morphological phenotypes of the proximal extraembryonic endoderm (VE, ME, and PE) of the *Sox17*-null conceptus isolated at 8.5–9.5 dpc (Figure 3). Since the PE and ME regions are frequently damaged in conventional isolation of the conceptus, we carried out serial sectioning analyses of whole-pregnant-uterus samples without any isolation of each conceptus in combination with genotyping by anti-SOX17 immunohistochemistry (Supplemental Figure S2).

In *Sox17*-null concepti at 8.5 dpc, HE staining revealed no appreciable histological defects in the extraembryonic endoderm of the VE, ME, and PE regions (control, n = 5; *Sox17*-null, n = 3; Figure 3A and B). The findings showed that, in both genotypes, proximal ME cells exhibited morphological characteristics intermediate between those of the VE and PE (inset of Figure 3A and B), in addition to widely spaced squamous cells in the PE region, even in *Sox17*-null concepti. In the wild-type and heterozygous concepti at 9.5 dpc, the proximal ME cells displayed hybrid VE/PE morphological characteristics at the junction between the PE and VE (inset in Figure 3C and E), which is consistent with the findings of previous morphological studies [5, 6]. Interestingly, in the *Sox17*-null littermates at 9.5 dpc, the prospective ME region significantly expanded toward the PE region (number of epithelial cells underneath the placental disk: 4.7 ± 1.3 cells in wild-type/heterozygote mutants versus 11.8 ± 1.6 cells in *Sox17*-null mutants; $p < 0.01$; control, n = 4; *Sox17*-null, n = 4), in which the ME cells displayed VE-like epithelial cell characteristics with cytoplasmic vacuole within the PE region (inset in Figure 3D and F). Moreover, in some severe cases, an ectopic VE-like epithelial cell patch was detectable in the PE region far from the marginal region (Supplemental Figure S3). The laminin-positive Reichert membrane underneath this ectopic GFP (SOX17)-positive epithelial cell patch was specifically thin in the PE region (Supplemental Figure S3), which is also consistent with the present findings showing aberrant expansion of the ME region in *Sox17*-null concepti.

VE-like characteristics in the presumptive ME region of *Sox17*-null but not *Sox7*-null concepti

Because the co-expression of *Sox17* and *Sox7* in the ME regions is observed by at least 7.5 dpc (Figure 2E), we established *Sox7* heterozygote lines with a loss-of-function mutation using the CRISPR/Cas9 system and comparatively examined the phenotypes

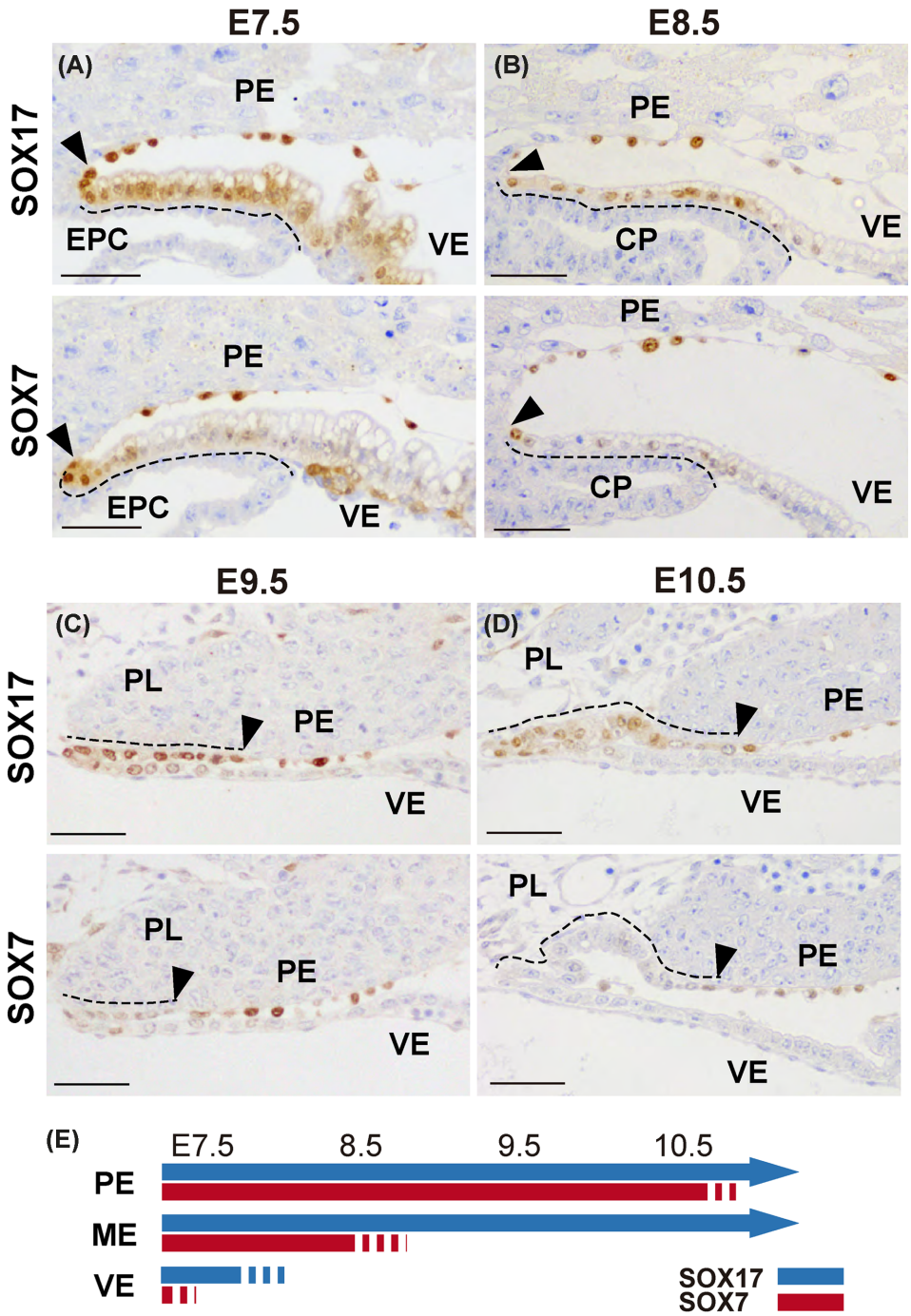

Figure 2. Comparative immunohistochemical analyses of SOX17 and SOX7 expression in the ME region. (A–D) Anti-SOX17 (upper plates) or -SOX7 (lower plates) immunohistochemistry (brown staining) of the marginal endoderm region at E 7.5 (A), E 8.5 (B), E 9.5 (C), and E 10.5 (D). (E) A schematic representation showing the expression profiles of SOX17 (blue) and SOX7 (red) in PE, ME, and VE regions. CP, chorionic plate; EPC, ectoplacental cone; PE, parietal endoderm; PL, placental disk; VE, visceral endoderm. Bar, 50 μm.

of the proximal extraembryonic endoderm adjacent to the placental disk in *Sox17*-null and *Sox7*-null concepti.

In wild-type concepti, the extraembryonic endoderm in the ME region, as well as the PE region, was negative for antihepatic nuclear factor 4, alpha (HNF4a; a VE marker) staining (Figure 4A and D). Moreover, at 9.5 dpc, the proximal VE region near the placental disk showed a lack or lower levels of HNF4a-positive signals, which is in sharp contrast to the high HNF4a expression in the distal VE region in the same wild-type conceptus. Such restricted HNF4a expression profiles in the distal VE region were very similar to those in the *Sox7*-null concepti (Figure 4C and F). In *Sox17*-null concepti, HNF4a-positive signals appeared to be increased in the ME region

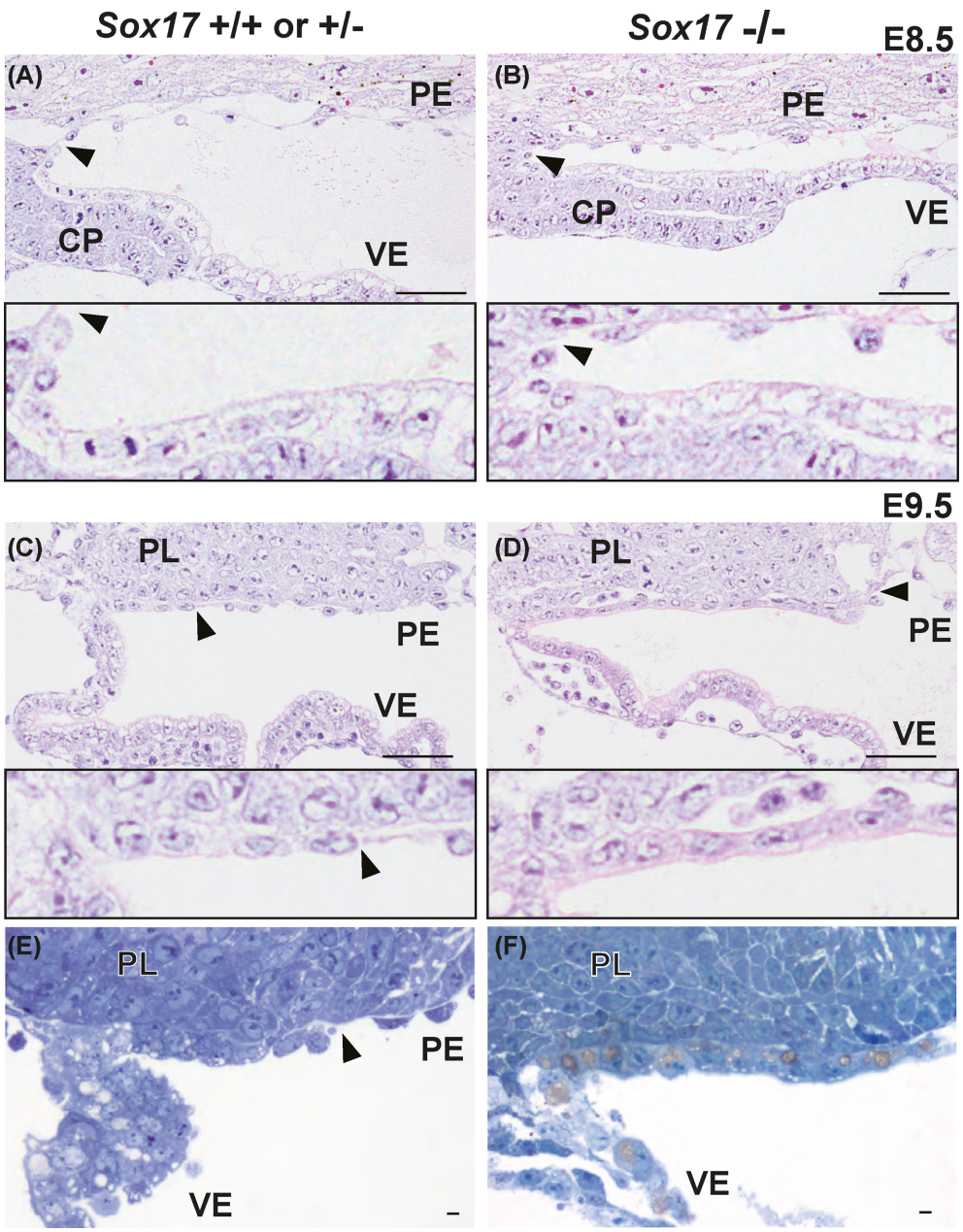

Figure 3. Ectopic appearance of VE-like epithelial cells in the ME region of *Sox17*-null concepti. HE staining (A–D) and toluidine-blue staining (E and F) of the VE, ME, and PE around the developing placental disk in the *Sox17*-null concepti; no appreciable histological defects can be observed in E8.5 (A and B), but an ectopic appearance of the VE-like epithelial cell layer can be seen in the presumptive ME region in E9.5 (C–F). Insets show higher magnification images of the proximal extraembryonic endoderm including the ME adjacent to the placental disk. Arrowheads mark the border of the PE and ME. CP, chorionic plate; PE, parietal endoderm; PL, placental disk; VE, visceral endoderm. Bar, 50 μm.

even at 8.5 dpc (control, n = 6; *Sox17*-null, n = 7; *Sox7*-null, n = 3; Figure 4B), albeit with no appreciable histological defects at this stage (Figure 3A and B). This HNF4a-positive domain was found to expand widely toward the PE and VE regions at 9.5 dpc (broken line and asterisk in Figure 4E), which is in sharp contrast to the restricted HNF4a-positive signals in only the distal VE region of *Sox7*-null concepti (control, n = 5; *Sox17*-null, n = 5; *Sox7*-null, n = 3; Figure 4F). Anti-CDH1 (an epithelial polarity marker) and antiphosphorylated-ezrin/radixin/moesin (p-ERM; an epithelial microvillus marker) staining confirmed their positive signals in the endoderm cells throughout the VE region; this was in contrast to their lack of expression in the PE region in the wild-type and *Sox7*-null concepti (control, n = 3; *Sox17*-null, n = 3; *Sox7*-null, n = 3; Figure 4G, I, J, and L). In *Sox17*-null concepti, CDH1/p-ERM-positive epithelial-like cells appeared to expand toward the presumptive PE region (broken lines in Figure 4H and K), and this was in contrast to those in wild-type and *Sox7*-null ones.

In all of the three (wild type, *Sox17*-null, and *Sox7*-null) concepti, the PE cells were positive for anti-GATA binding protein 6 (GATA6) staining (Figure 4M–R). Several ME cells showed considerable, albeit weak, positivity for anti-GATA6 staining, especially in the region close to the PE region in the wild-type (Figure 4M and P)

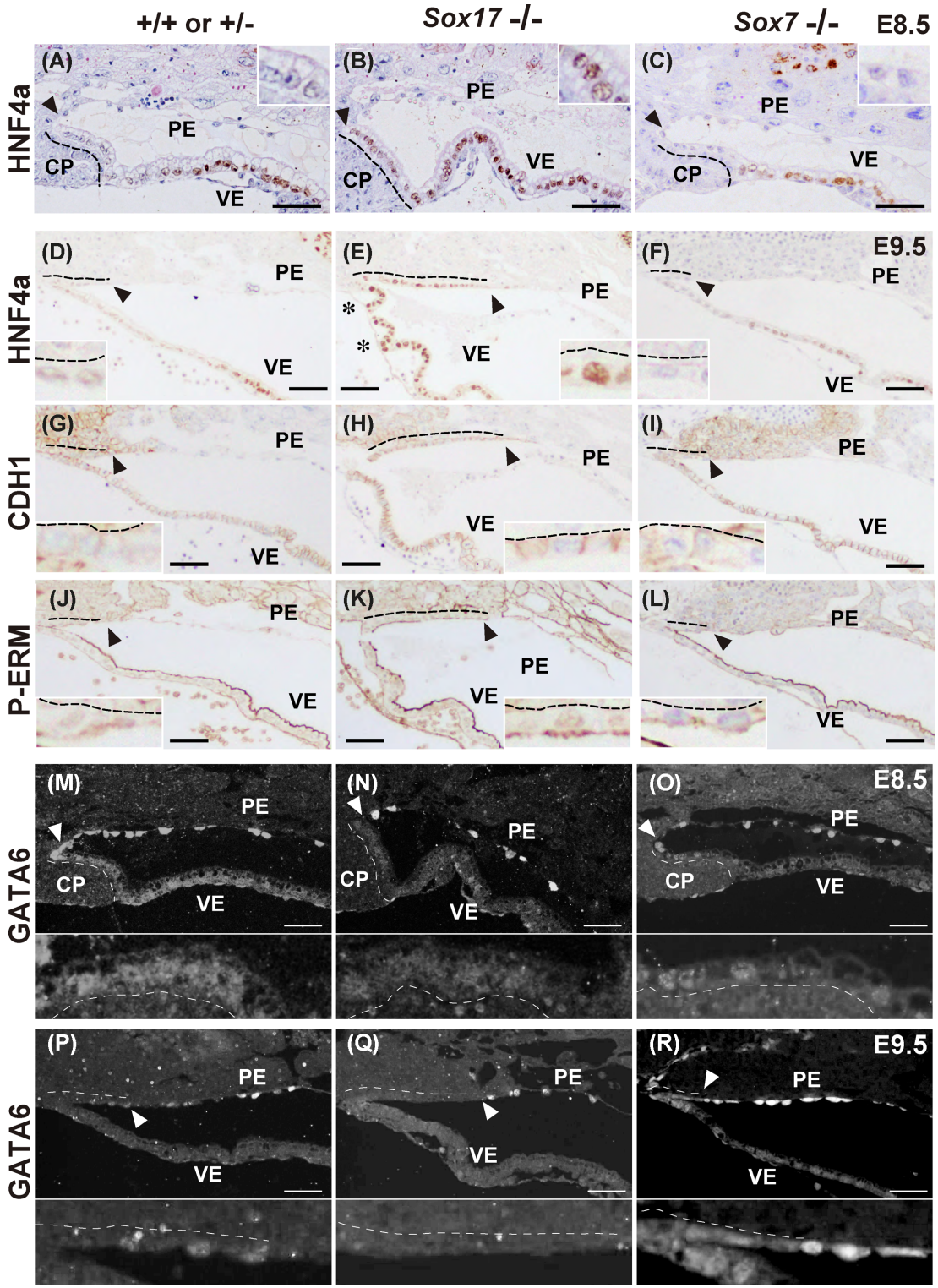

Figure 4. Immunohistochemical analyses of the expression profiles of VE and PE markers in the ME region of *Sox17*- or *Sox7*-null concepti. Comparative expression profiles of VE (HNF4a, CDH1 [an epithelial cell polarity marker], and p-ERM [an epithelial microvillus marker]) and PE (GATA6) markers using serial sections of the ME region of the wild-type/heterozygote (left column; A, D, G, J, M, P), *Sox17*-null (middle column; B, E, H, K, N, Q), and *Sox7*-null concepti (right column; C, F, I, L, O, R). Arrowheads mark the proximal end of the PE region, whereas broken lines indicate the presumptive ME region adjacent to placental tissues. Insets show higher magnification images of the ME region. CP, chorionic plate; PE, parietal endoderm; VE, visceral endoderm. Bar, 50 μm.

and *Sox7*-null concepti (Figure 4O and R). Interestingly, the *Sox17*-null concepti showed high levels of GATA6 expression in PE cells, but no detectable GATA6-positive signals were observed in the ME region (control, n = 3; *Sox17*-null, n = 3; *Sox7*-null, n = 3; Figure 4N and Q). These findings indicate that the ME cells were originally in an HNF4a-negative/GATA6-low state in wild-type concepti and that they were widely replaced by HNF4a-high/GATA6-negative epithelial cells similar to those in the distal VE region in *Sox17*-null ones.

Aberrant ME phenotypes of *Sox17*-null concepti could not be rescued by injection of *Sox17*$^{+/+}$ ES cells into blastocysts

Sox17-null concepti showed deficiency of gut endoderm and the lack of axis rotation, and died by 10.5 dpc. To examine the possible contribution of defective gut endoderm formation to aberrant ME phenotypes of *Sox17*-null concepti [9, 24, 26], wild-type ES cells were injected into *Sox17*-null blastocysts, and then the phenotypes of the *Sox17*-null concepti including *Sox17*$^{-/-}$ < − > wild-type (GFP) chimeric embryos were analyzed (Figure 5A). Among a total of 27 concepti, we successfully obtained one chimeric conceptus with proper embryonic turning of the body trunk that occurred together with the high contribution of wild-type ES-derived (GFP^{+}) gut endoderm (Figure 5C and E). The *Sox17*$^{-/-}$ < − > wild-type (GFP) chimeric embryo showed a moderate contribution of *Sox17*$^{+/+}$ ES (GFP^{+}) cells to embryonic tissues, including the GFP^{+} hindgut epithelium (lower right inset in Figure 5C), with no contribution of the GFP-positive ES cells to the extraembryonic endoderm layers (upper left inset in Figure 5C). Anti-HNF4a and anti-GFP immunostaining revealed ectopic HNF4a expression in GFP-negative ME and proximal VE regions in this conceptus (Figure 5E), which is in contrast to the lack of HNF4a expression in those of the control *Sox17*$^{+/-}$ < − > wild-type (GFP) chimeric concepti (Figure 5B and D). Although there was a milder phenotype in the ME region (i.e. ectopic expansion of the VE-like region) in this chimeric conceptus, we concluded that there was no appreciable recovery of the defective *Sox17*-null phenotype in the ME region upon rescue of the chimeric embryo by the injection of wild-type ES cells into the blastocyst.

Mild defects in cell proliferation and shape in PE cells of *Sox17*-null concepti

The density of PE cells in *Sox17*-null concepti was compared with that in their wild-type/heterozygous littermates by using sections of the whole uterus (Figure 6A). At 8.0 dpc, the relative number of PE cells per Reichert membrane length showed no significant differences in the PE region between the *Sox17*-null and wild-type/heterozygous littermates. However, at 8.5 dpc, the relative PE cell number was significantly, albeit slightly, reduced in the *Sox17*-null concepti compared with the level in wild-type/heterozygous littermates ($p < 0.05$; middle bars in Figure 6A). This is in contrast to the lack of appreciable changes in the cell density of *Sox7*-null and wild-type/heterozygous littermates (right column in Figure 6A). EdU-positive indices in PE cells, but not in VE cells, were also reduced in *Sox17*-null concepti compared with the level in the wild-type/heterozygote littermates, at 8.5 dpc (Figure 6B).

Finally, PE cells with Reichert membrane were isolated from the *Sox17*-null (*Gfp*/*Gfp*) and *Sox17*-heterozygote (*Gfp*/+) concepti, and their cell shapes were then examined and compared under a fluorescent microscope (Figure 6C and D). The *Sox17*-null PE cells showed spreading cell shapes in contrast to the round shape of heterozygote PE cells. Morphometric analyses confirmed a significant increase in the number of cell processes of PE cells in *Sox17*-null concepti compared with that in normal (heterozygote) ones ($p < 0.05$; n = 4). These findings indicate the presence of mild but clear defects in PE cells, as well as in ME cells, in *Sox17*-null concepti.

Discussion

Several previous studies demonstrated the coexpression of SOX17 and SOX7 in PrE and its derivatives, PE and VE, at least by the late stages of gastrulation (~7.75 dpc; [9, 11]). The present study extended these previous findings to the expression profiles at later stages and demonstrated that SOX17, but not SOX7, is continuously expressed in the ME adjacent to the developing placental disk (Figures 1 and 2). Moreover, the present study revealed that the ME region of *Sox17*-null concepti displays an ectopic and aberrant expansion of VE-like epithelia along the marginal edge of the developing placental disk at and after 8.5 dpc, which is in sharp contrast to the lack of appreciable defects in the ME region of *Sox7*-null concepti at the same stage. These findings indicate that *Sox17*, not *Sox7*, plays a crucial role in the proper formation and/or maintenance of the ME region in mouse placental formation.

The marginal extraembryonic endoderm adjacent to the developing placental disk shows a gradient hybrid character of PE/VE cell morphology at the junction between them [6]. In the narrow ME region, VE-like cells are located at the most VE side, whereas PE-like cells are seen at the most PE side; there is a gradient of alteration of each cell morphology from the VE to the PE in the intermediate region ([6]; Figure 3E). This gradient hybrid character of ME may be explained by the gradated expression of SOX17/SOX7/GATA6 signals in this region (Figures 2 and 4 M-O, Supplemental Figure S2C) in addition to a reduction in and/or lack of HNF4a signals in the proximal VE region in the wild-type concepti (Figure 4A–F).

By using in vitro experiments on the extraembryonic endoderm, it was previously shown that isolated VE cells directly contacting with extraembryonic ectoderm at early gastrulation stages were able to undergo morphological transformation from VE to PE-like cells in vitro [7], suggesting the possible maintenance of the capacity to perform VE-to-PE conversion in early-stage VE cells [7]. Interestingly, it has been reported that such VE-to-PE transdifferentiation potency rapidly decreased in the distal VE region during 7.5–8.5 dpc, if the VE has been kept lined with extraembryonic mesoderm [7], leading to a distal-to-proximal loss of the transdifferentiation potency in the VE region during this period. In the present study, SOX17 expression was observed in a wider part of the proximal extraembryonic VE region at 6.5–7.5 dpc, but this expression rapidly became restricted to the proximal site of the VE (i.e. ME) by 8.5 dpc. These findings imply that such a loss of VE-to-PE transdifferentiation potency in the extraembryonic VE region may be positively associated with the reduction of SOX17 expression in a distal-to-proximal manner after 7.5 dpc in vivo. It was previously reported that SOX17 was able to repress *Hnf4a* expression level through the actions of its direct target gene, *Zfp202,* in F9 endoderm differentiation [27]. Furthermore, it has been reported that HNF4a orchestrates the expression of cell junction and adhesion proteins including CDH1 in the epithelialization of the hepatocyte [28]. From these preceding studies, SOX17 appears to negatively regulate the epithelial polarization of the extraembryonic endoderm partially through the repression of HNF4a expression, which subsequently leads to the VE to PE transdifferentiation in the ME region.

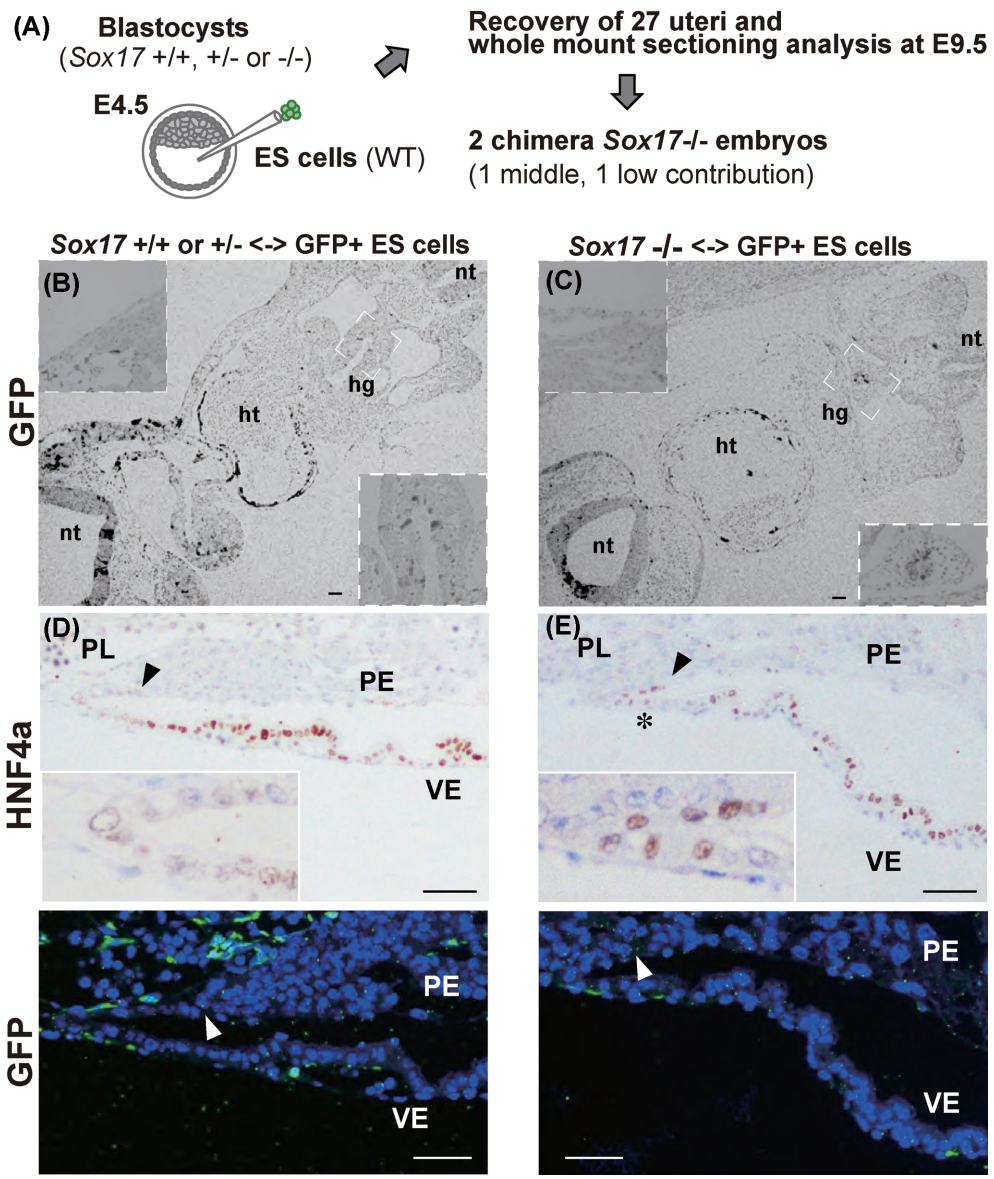

Figure 5. A rescue experiment in *Sox17*-null conceptus by injection of wild-type ES cells into blastocyst. (A) Schematic representation showing the production of chimeric concepti by the injection of wild-type (GFP^+) ES cells into blastocysts that were obtained by crossing $Sox17^{+/-}$ parents (left). Among 27 concepti, only two $Sox17^{-/-} < - >$ wild-type (GFP^+) chimeric concepti were obtained at 9.5 dpc. (B–E) The wild-type (GFP^+) ES cells moderately contributed to control (B) and $Sox17^{-/-}$ (C) chimeric embryos. In C, the $Sox17^{-/-} < - >$ wild-type chimeric embryo displays proper embryonic turning together with a high contribution of GFP^+ wild-type cells to the hindgut endoderm (lower right inset in C). Neither chimeric conceptus showed a contribution of GFP^+ wild-type cells to the VE, ME, or PE (upper inset in the top plate of B, C; GFP plates in D, E). No appreciable defects were detectable in the ME region of the control (D). hg, hind gut; ht, heart; nt, neural tube; PE, parietal endoderm; PL, placental disk; VE, visceral endoderm. Arrows head mark the borders of the ME. Bar, 50 μm.

The ME cells did not appear to proliferate actively compared with the VE and PE cells at 8.5 dpc ([8]; our unpublished data), suggesting that they are a minor source of the supply of the extraembryonic endoderm cells of the PE and VE. However, it was previously speculated that the proximal VE cells may relocate toward the PE side via the marginal zone, which results in their partial contribution to PE cells at the gastrulation stage [6, 7]. This is also consistent with previous labeling tracing data showing the tendency of proximal VE cells to migrate in the proximal direction (toward the placental disk) in whole-embryo culture [29].

In the *Sox17*-null concepti, the ME region appeared to expand toward the PE side (Figures 3D and 4E). In certain severe cases, VE-like epithelial cell patches were ectopically found within the PE region (Supplemental Figure S3). Artus [11] demonstrated that aberrant immature PE cells relocated from the inner cell mass region to the TE side in the 3-day culture of *Sox17*-null blastocysts, similar to the aberrant spreading of the cell shapes of *Sox17*-null PE cells on Reichert membrane (Figure 6C and D). With regard to these findings, it is possible that, even at later stages of organogenesis, SOX17-positive ME cells relocate and contribute to PE cells near the chorionic plate and that such aberrant formation of VE-like epithelia may be caused by defects in VE-to-PE transformation in the ME region of *Sox17*-null concepti. Interestingly, the ME region was previously shown to contribute to the intraplacental yolk sac, a tissue crucial for

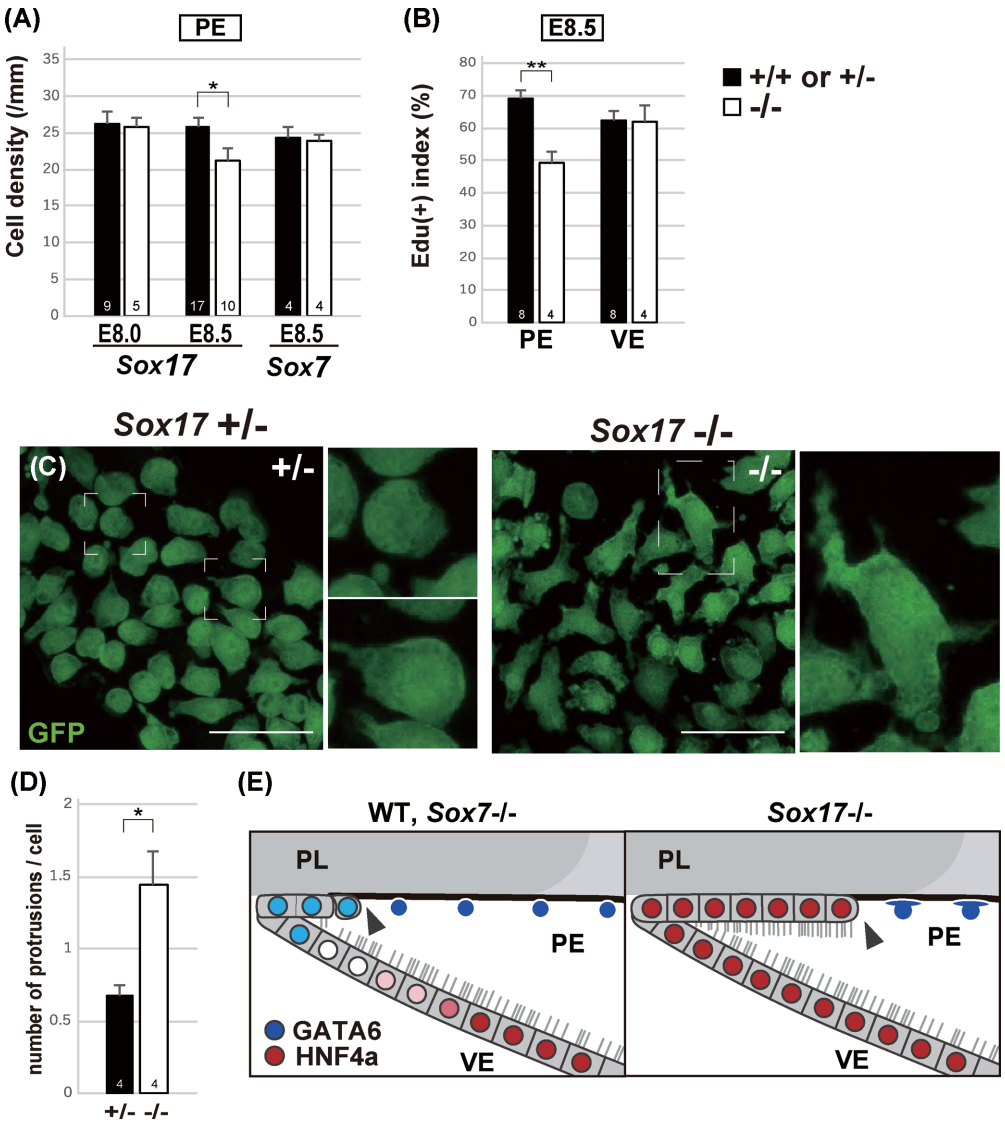

Figure 6. Morphometric analyses of cell density, proliferation, and shape of PE cells in *Sox17*-null concepti. (A) Morphometric analyses using whole-uterus sections showing a slight but significant reduction of the density of PE cells (i.e. cell number per mm length of basal lamina membrane) in *Sox17*-null concepti compared with that in the neighboring wild-type/heterozygote littermates at 8.5 dpc. No defect in the density of PE cells was detectable in *Sox7*-null concepti at 8.5 dpc. (B) Bar graphs showing EdU-positive indices in the PE and VE regions of the *Sox17* wild-type/heterozygous and *Sox17*-null concepti at 8.5 dpc (note a significant reduction in the PE but not in the VE). (C and D) GFP-fluorescent image (C) showing the shape of a whole PE cell on Reichert membrane, whereas the bar graph (D) shows the number of cell processes per PE cell in $Sox17^{+/-(+/Gfp)}$ and $Sox17^{-/-(Gfp/Gfp)}$ concepti at 8.5 dpc. Arabic numerals inside the bar indicate the number of samples used. (E) Schematic representation showing the phenotypes of the ME region in the *Sox7*-null concepti during placental development. ME cells were originally in an HNF4a-negative/GATA6-low (light blue) state in wild-type and *Sox7*-null concepti, whereas they were widely replaced by HNF4a-high (red)/GATA6-negative epithelial cells, similar to those in the distal VE region. GATA6-positive PE cells are colored dark blue, whereas epithelial cells are decorated with apical microvilli. PE, parietal endoderm; PL, placental disk; VE, visceral endoderm. Bar, 50 μm.

maternal–fetal calcium transport, throughout pregnancy ([30]; and references therein). Further studies on the roles of SOX17 and SOX7 in the ME region and its derivatives are required to obtain a better understanding of the function and biological significance of this region in mouse placentation.

In conclusion, the present study is the first to demonstrate a crucial role of SOX17 in the formation and maintenance of the ME with a gradient hybrid character of PE/VE cell morphology at the junction between two yolk-sac membranes. It also provides important molecular and cellular insights into the regionalized VE–PE transition in the marginal edge of developing mouse placenta in vivo.

Supplementary data

Supplementary data are available at *BIOLRE* online.

Figure S1. Establishment of three *Sox7*-mutant mouse lines by CRISPR-Cas9. (A) Schematic representation of the coding region of the murine *Sox7* gene. Its DNA binding HMG-box domain is indicated in blue. Amino acid sequences of the wild-type and three independent lines with frame-shift mutations of *Sox7* (4-, 28-, or 31-bp deletion just upstream of the first alpha helices of the HMG box domain). Predicted amino acid sequences caused by frame-shift mutations are written in red (asterisk, stop codon). (B and C) Whole-mount images of wild-type, *Sox7*-heterozygote, and *Sox7*-null

littermates and their isolated embryos at 10.5 dpc. *Sox7*-null conceptus showed the typical phenotypes of a lack of large blood vessels in the yolk sac (B) and severe embryonic growth retardation (C). Bar, 1mm.

Figure S2. Whole-pregnant-uterus analysis and immunohistochemical genotyping. (A and B) Schematic representation (A) and HE staining images (B) of serial sections of the whole-mount pregnant uterus sample. The whole uterus was dissected into each two-conceptus part of the whole uterine tube, followed by direct fixing with Bouin solution or 4% PFA-PBS for preparation of the paraffin sections. (C, D) Each genotype of the conceptus within the fixed whole-uterus samples was estimated by anti-SOX17 or -SOX7 immunostaining in the PE region of each conceptus. The presence (wild type or +/−) or absence (−/−) of SOX17- or SOX7-positive signals was monitored in the PE cells of each conceptus (C, D), in addition to reference staining: anti-GFP signals (*Sox17*-null allele) in $Sox17^{+/-\,(+/Gfp)}$ or $Sox17^{-/-\,(Gfp/Gfp)}$ conceptus (lower sections in C) and positive control of GATA6 in PE cells (lower plates in D). In all of the whole-pregnant-uterus samples, either the heterozygote/wild-type or the null genotype was also reconfirmed by the absence or presence of the typical phenotypes of the *Sox17*-null (no axis rotation; see also the embryo on the right side in B) or *Sox7*-null embryos (growth-retarded embryos with no large blood vessels). PE, parietal endoderm; VE, visceral endoderm. Bar, 50 μm.

Figure S3. A severe case of *Sox17*-null conceptus showing ectopic epithelial cell sheet in the PE region. (A–C) HE and anti-GFP (green) and anti-laminin (red) staining images of the PE region far from the proximal VE region in the $Sox17^{-/-(GFP/GFP)}$ conceptus. The GFP-positive epithelial cell sheet (arrowheads) is positioned within the PE region underneath a thin layer of laminin-positive Reichert membrane. Arrows mark the borders of the expanded ME region. ME, marginal zone endoderm; PE, parietal endoderm; PL, placental disk; VE, visceral endoderm. Bar, 50 μm.

Supplementary Table 1 List of antibodies used in this study

Acknowledgments

The authors wish to thank Dr Youichirou Ninomiya (National Institute of Informatics) for his kind critical reading on the manuscript.

References

1. Gardner RL, Papaioannou VE. Differentiation in the trophectoderm and inner cell mass. In Balls M, Wild AE (eds.), *Early Development Mammals* 1st ed. Cambridge: Cambridge University Press; 1975:107–132.
2. Gardner RL, Rossant J. Investigation of the fate of 4-5 day post-coitum mouse inner cell mass cells by blastocyst injection. *J Embryol Exp Morphol* 1979; **52**:141–152.
3. Gardner RL. Investigation of cell lineage and differentiation in the extraembryonic endoderm of the mouse embryo. *J Embryol Exp Morphol* 1982; **68**:175–198.
4. Gardner RL. An in situ cell marker for clonal analysis of development of the extraembryonic endoderm in the mouse. *J Embryol Exp Morphol* 1984; **80**:251–288.
5. Hogan BL, Newman R. A scanning electron microscope study of the extraembryonic endoderm of the 8th-day mouse embryo. *Differentiation* 1984; **26**:138–143.
6. Hogan BL, Tilly R. Cell interactions and endoderm differentiation in cultured mouse embryos. *J Embryol Exp Morphol* 1981; **62**:379–394.
7. Ninomiya Y, Davies TJ, Gardner RL. Experimental analysis of the trans-differentiation of visceral to parietal endoderm in the mouse. *Dev Dyn* 2005; **233**:837–846.
8. Kunath T, Rossant J. Stem cells in extraembryonic lineages. In: Lanza R, Gearhart J, Hogan B, Melton D, Pedersen R, Thomas J, Thomas ED, West M (eds.), *Essentials of Stem Cell Biology*, 2nd ed. San Diego: Elsevier Academic Press; 2009:117–125.
9. Kanai-Azuma M, Kanai Y, Gad JM, Tajima Y, Taya C, Kurohmaru M, Sanai Y, Yonekawa H, Yazaki K, Tam PP, Hayashi Y. Depletion of definitive gut endoderm in Sox17-null mutant mice. *Development* 2002; **129**:2367–2379.
10. Frankenberg S, Gerbe F, Bessonnard S, Belville C, Pouchin P, Bardot O, Chazaud C. Primitive endoderm differentiates via a three-step mechanism involving Nanog and RTK signaling. *Dev Cell* 2011; **21**:1005–1013.
11. Artus J, Piliszek A, Hadjantonakis AK. The primitive endoderm lineage of the mouse blastocyst: sequential transcription factor activation and regulation of differentiation by Sox17. *Dev Biol* 2011; **350**:393–404.
12. Kinoshita M, Shimosato D, Yamane M, Niwa H. Sox7 is dispensable for primitive endoderm differentiation from mouse ES cells. *BMC Dev Biol* 2015:**15**:37.
13. Shimoda M, Kanai-Azuma M, Hara K, Miyazaki S, Kanai Y, Monden M, Miyazaki J. Sox17 plays a substantial role in late-stage differentiation of the extraembryonic endoderm in vitro. *J Cell Sci* 2007; **120**:3859–3869.
14. Lim CY, Tam WL, Zhang J, Ang HS, Jia H, Lipovich L, Ng HH, Wei CL, Sung WK, Robson P, Yang H, Lim B. Sall4 regulates distinct transcription circuitries in different blastocyst-derived stem cell lineages. *Cell Stem Cell* 2008; **3**:543–554.
15. Cho LT, Wamaitha SE, Tsai IJ, Artus J, Sherwood RI, Pedersen RA, Hadjantonakis AK, Niakan KK. Conversion from mouse embryonic to extra-embryonic endoderm stem cells reveals distinct differentiation capacities of pluripotent stem cell states. *Development* 2012; **139**:2866–2877.
16. McDonald AC, Biechele S, Rossant J, Stanford WL. Sox17-mediated XEN cell conversion identifies dynamic networks controlling cell-fate decisions in embryo-derived stem cells. *Cell Reports* 2014; **9**:780–793.
17. Kim I, Saunders TL, Morrison SJ. Sox17 dependence distinguishes the transcriptional regulation of fetal from adult hematopoietic stem cells. *Cell* 2007; **130**:470–483.
18. Fujihara Y, Kaseda K, Inoue N, Ikawa M, Okabe M. Production of mouse pups from germline transmission-failed knockout chimeras. *Transgenic Res* 2013; **22**:195–200.
19. Hashimoto M, Takemoto T. Electroporation enables the efficient mRNA delivery into the mouse zygotes and facilitates CRISPR/Cas9-based genome editing. *Sci Rep* 2015; **5**:11315.
20. Kim K, Kim IK, Yang JM, Lee E, Koh BI, Song S, Park J, Lee S, Choi C, Kim JW, Kubota Y, Koh GY, et al. SoxF Transcription Factors Are Positive feedback regulators of VEGF signaling novelty and significance. *Circ Res* 2016; **119**:839–852.
21. Lilly AJ, Costa G, Largeot A, Fadlullah MZ, Lie-A-Ling M, Lacaud G, Kouskoff V. Interplay between SOX7 and RUNX1 regulates hemogenic endothelial fate in the yolk sac. *Development* 2016; **143**:4341–4351.
22. Lilly AJ, Mazan A, Scott DA, Lacaud G, Kouskoff V. SOX7 expression is critically required in FLK1-expressing cells for vasculogenesis and angiogenesis during mouse embryonic development. *Mech Dev* 2017; **146**:31–41.
23. Sakamoto Y, Hara K, Kanai-Azuma M, Matsui T, Miura Y, Tsunekawa N, Kurohmaru M, Saijoh Y, Koopman P, Kanai Y. Redundant roles of Sox17 and Sox18 in early cardiovascular development of mouse embryos. *Biochem Biophys Res Commun* 2007; **360**:539–544.
24. Saund RS, Kanai-Azuma M, Kanai Y, Kim I, Lucero MT, Saijoh Y. Gut endoderm is involved in the transfer of left-right asymmetry from the node to the lateral plate mesoderm in the mouse embryo. *Development* 2012; **139**:2426–2435.
25. Matsui T, Kanai-Azuma M, Hara K, Matoba S, Hiramatsu R, Kawakami H, Kurohmaru M, Koopman P, Kanai Y. Redundant roles of Sox17 and Sox18 in postnatal angiogenesis in mice. *J Cell Sci* 2006; **119**:3513–3526.
26. Viotti M, Niu L, Shi SH, Hadjantonakis AK. Role of the gut endoderm in relaying left-right patterning in mice. *PLoS Biol* 2012; **10**: e1001276.

27. Patterson ES, Addis RC, Shamblott MJ, Gearhart JD. SOX17 directly activates Zfp202 transcription during in vitro endoderm differentiation. *Physiol Genomics* 2008; **34**:277–284.
28. Battle MA, Konopka G, Parviz F, Gaggl AL, Yang C, Sladek FM, Duncan SA. Hepatocyte nuclear factor 4 orchestrates expression of cell adhesion proteins during the epithelial transformation of the developing liver. *Proc Natl Acad Sci* 2006; **103**:8419–8424.
29. Takaoka K, Yamamoto M, Hamada H. Origin and role of distal visceral endoderm, a group of cells that determines anterior–posterior polarity of the mouse embryo. *Nat Cell Biol* 2011; **13**:743–752.
30. Suzuki Y, Kovacs CS, Takanaga H, Peng JB, Landowski CP, Hediger MA. Calcium channel TRPV6 is involved in murine maternal-fetal calcium transport. *J Bone Miner Res* 2008; **23**:1249–1256.